Available online at www.sciencedirect.com

ScienceDirect

Procedia Structural Integrity 25 (2020) 254–261

Structural Integrity Procedia

www.elsevier.com/locate/procedia

1st Virtual Conference on Structural Integrity - VCSI1

Model for fatigue crack growth analysis

MF Borges*[a], FV Antunes[a], P Prates[a], R Branco[a], J.M. Vasco-Olmo[b], F.A. Díaz[b]

[a] *CEEMPRE, Department of Mechanical Engineering, University of Coimbra, Portugal*
[b] *Departamento de Ingeniería Mecánica y Minera, University of Jaén, Jaén, Spain*

Abstract

The application of damage tolerance to the design of components is based on the ability to predict fatigue crack growth (FCG) rate precisely. A literature review about analytical models showed a great number of models developed for specific materials and loading conditions. A numerical analysis of a CT specimen made of 304L stainless steel showed the complex influence of material parameters on FCG, which also depends on loading parameters, geometry and environmental conditions. Therefore an alternative to analytical models is proposed here, based on plastic CTOD, assuming that this is the crack driving force. A material law must be first obtained relating da/dN with plastic CTOD range, δ_p, obtained numerically using the finite element method or experimentally using DIC. This law changes with material and includes all material parameters and also environmental conditions (temperature and atmosphere). The design of a specific cracked component is made using numerical tools in order to obtain δ_p for different crack lengths. This second analysis includes the effect of geometrical and loading parameters.

Keywords: Fatigue crack growth; Analytical models; Crack Tip Opening Displacement (CTOD)

1. Introduction

Designers are pressed to reduce the level of conservatism in engineering systems in order to meet targets on cost, weight and emissions. Prediction of remaining life of the structural elements influences the decisions of maintenance

* Corresponding author. Tel.:00351 239790706; fax: 00351-239790701.
E-mail address: micaelfriasborges@outlook.pt

2452-3216
10.1016/j.prostr.2020.04.030

engineers (checking intervals, corrections, replacements). Most of the industries now-a-days prefer to follow the damage tolerance approach. Such an approach involves designing of structural components with certain allowance to small cracks (i.e. the non-propagating cracks) or the defects, which could be repaired from time to time by periodic inspection. Non-destructive techniques are generally used to analyze and evaluate the residual fatigue life of the components. This approach is particularly recommended for manufacturing industries where defects are unavoidable such as the case of welding, casting or additive manufacturing. The ability to model and predict fatigue crack growth rate precisely is one of the key aspects of the damage tolerance approach. There is a great number of models and approaches for fatigue crack growth analysis, and the selection of the model is usually based on the experience and persona1 preference of the analyst.

The objectives of the present study are (1) to present literature models; (2) to present numerical results about the effect of material parameters on fatigue crack growth (FCG) and (3) to promote a discussion about the FCG models. The parameters studied in the numerical approach were Young's modulus, yield stress, Y_0, and isotropic and kinematic hardening parameters. The challenge is a model which includes all parameters and is dimensionally consistent.

2. Literature review

2.1. Models with load parameters

Table 1. FCG models with loading parameters.

Reference	Model	Comments
Paris	$\frac{da}{dN} = C\Delta K^m$	C, m - constants
Forman (1967)	$\frac{da}{dN} = \frac{C\Delta K^m}{(1-R)K_c - \Delta K}$	0<R<1 R – stress ratio K_c – Fracture toughness
Erdogan and Ratwani (1970)	$\frac{da}{dN} = \frac{C(1+\beta)^m(\Delta K - \Delta K_{th})^m}{K_C - (1+\beta)\Delta K}$	$\beta = \frac{K_{max} + K_{min}}{K_{max} - K_{min}}$
Raju (1972)	$\frac{da}{dN} = \frac{C(1-R)^{4-m} K_{max}^4}{K_C - K_{max}^4}$	
NASGRO (2016)	$\frac{da}{dN} = C\left(\frac{1-f}{1-R}\Delta K\right)^n \frac{(1-\Delta K_{th}/\Delta K)^p}{(1-\Delta K_{max}/K_c)^q}$	f – crack opening function for crack closure C, n, p, q - material constants
Kwofie and Rabar (2011)	$\frac{da}{dN} = C\,\Delta K_R^m$ $\Delta K_R = \Delta K_{eq} \exp\left(-\alpha\left(\frac{1+R}{1-R}\right)\right)$	α - mean stress sensitivity factor
Walker (1970)	$\frac{da}{dN} = C\left(\frac{\Delta K}{(1-R)^n}\right)^m$	
Kujawski (2001)	$\frac{da}{dN} = CK_{max}^{\alpha}(\Delta K^+)^{1-\alpha}$	$0 \le \alpha \le 1$ quantifies the sensitivity to K_{max} ΔK^+ - positive range of ΔK

A very large number of models have been proposed to describe FCG dealing with loading parameters. Table 1 presents some of these models. The first model was Paris law, which assumed that ΔK is the crack driving force. Fatigue threshold, ΔK_{th}, and fracture toughness, K_C, were added to the models in order to define the lower and upper limits of da/dN-ΔK curves, respectively. In order to include the effect of stress ratio, R, which increases FCG rate for the same ΔK, Elber proposed the crack closure phenomenon and an effective $\Delta K=K_{max}-K_{open}$, being K_{max} and K_{open} the maximum and opening stress intensity factors (NASGRO, 2016). There are authors who disagree about the relevance of crack closure phenomenon and proposed alternative models to quantify the effect of stress ratio, like Walker (1970) or Kujawski (2001). All these models have fitting parameters and assume a deterministic behavior. Since they do not include material properties, they are specific for each material.

Table 2. FCG models including material parameters.

Reference	Model	Comments
Pelloux (1970)	$\frac{da}{dN}=\frac{2\Delta K^2}{\pi E Y_0}$	
Nicholls (1994)	$\frac{da}{dN}=\frac{\Delta K^4}{4EY_0K_c^2}$	
Schwalbe (1974)	$\frac{da}{dN}=\beta\frac{\Delta K^2}{4\pi(1+n)Y_0^2}\left(\frac{2Y_0}{\varepsilon_f E}\right)^{1+n}$	ε_f – failure strain n – hardening exponent
Jablonski (1977)	$\frac{da}{dN}=\frac{0.0338(1-\nu^2)}{\varepsilon_f EY_0}\Delta K^2$	
Chand and Garg (1985)	$\frac{da}{dN}=\frac{0.15\Delta K_{eff}^2 Y_0}{nEK_{Ic}^2(1+R)^{3.8}}$	
Skelton (1988)	$\frac{da}{dN}=\frac{\Delta K^2(1-\nu)}{2\pi EW_c}$	W_c – critical value of density of cumulative energy
Clavel and Pineau (1982)	$\frac{da}{dN}=\beta\frac{\Delta K^2}{EY_0}$	β=0.25
Shi (2014)	$\frac{da}{dN}=\frac{\Delta K_{eq}^2}{4\pi(1+n')\sigma_{ys}^2 N^*}$ $\Delta K_{eq}=(\Delta K-\Delta K_{th})^{1/2}$ $N^*=\frac{1}{2}\left(\frac{K'}{(\sigma_f'-\sigma_m)\varepsilon_f'}\right)\left(\frac{Y_0}{E}\right)^{n'+1}$	K'- cyclic strain hardening coefficient n' - cyclic strain hardening exponent

However, material properties have a significant influence on FCG rate, therefore material constants were included in the models, as indicated in Table 2. Concerning Young's modulus, E, there is an almost general agreement that da/dN is proportional to 1/E. The models of Schwalbe (1974) and Shi (2014) proposed other relations. Poisson ration, ν, is usually neglected, except in the models of Jablonski (1977) and Skelton (1988). Material's yield stress, Y_0, is widely included, and da/dN is assumed to be proportional to $1/Y_0$, in most of the models. However, other relations were proposed by Schwalbe (1974) and Shi (2014). The isotropic hardening is included in some of the models usually using the hardening exponent, n (or n', the cyclic hardening exponent). The kinematic hardening parameters were not included in literature models. There is also an influence of environment, namely temperature and atmosphere, which usually is not included in the models. Testing in vacuum shows the great influence of environment on FCG rate, which is usually associated with oxidation or hydrogen embrittlement. Therefore, all these models are incomplete in the sense that do not include all parameters affecting FCG.

3. Numerical model

A compact tension specimen, C(T), with a width, W, equal to 50 mm, and an initial crack length, a_0, of 24 mm, was numerically modeled in the DD3IMP, an in-house code. The symmetry conditions of specimen's geometry allowed the modeling of only ¼ of the specimen, reducing the numerical overhead. The contact of crack flanks enabled the simulation of plasticity induced crack closure. Relatively to the specimen's thickness, t, only 0.1 mm were simulated to reduce numerical effort and to obtain plane stress state. A remote cyclic load was applied in the hole of the specimen giving K_{max} and ΔK of 18.3 and 16.5 MPa.m$^{0.5}$, respectively, and a stress ratio R=0.1.

The finite element mesh was refined in the crack tip region, having there elements with 8×8 μm^2. Each crack increment corresponded to the dimension of the elements in the ultra-refined region (8 μm). Two load cycles were applied between crack increments. The total crack growth was 1.272 mm, which corresponded to 159 crack increments of 8 μm each, in order to stabilize tip plastic deformation and closure phenomenon. All simulations were evaluated at the first node behind the crack tip, at a distance of 8 μm.

The material behavior was simulated considering generalized Hooke's law for the elastic behavior, von Mises yield criterion and mixed (isotropic+kinematic) hardening, coupled with Voce isotropic hardening law:

$$Y = Y_0 + (Y_{Sat} - Y_0)[1 - exp(-C_Y \bar{\varepsilon}^p)] \tag{1}$$

and Frederick-Armstrong kinematic hardening law:

$$\dot{\boldsymbol{X}} = C_X \left[X_{Sat} \frac{\Sigma}{\bar{\sigma}} - \boldsymbol{X}' \right] \dot{\bar{\varepsilon}}^p, \tag{2}$$

Y_{Sat} is the isotropic saturation stress, C_Y is the isotropic saturation rate, $\bar{\varepsilon}^p$ is the equivalent plastic strain, $\dot{\boldsymbol{X}}$ is the back stress rate, $\bar{\sigma}$ is the equivalent stress, $\dot{\bar{\varepsilon}}^p$ is the equivalent plastic strain rate and C_X and X_{Sat} are the kinematic hardening parameters, respectively representing the saturation rate and the saturation value of the exponential kinematic hardening. Two materials were considered in this study, the 304L stainless steel and the 7050-T6 aluminium alloy. The material properties are presented in Table 3.

Table 3. FCG models including material parameters.

Reference	E [GPa]	ν [-]	Y_0 [GPa]	Y_{Sat} [MPa]	C_Y [-]	X_{Sat} [MPa]	C_Y [-]
SS304L	196	0.3	117	204	9	176	300
AA7050-T6	71.7	0.33	420.50	420.50	0	198.35	228.91

4. Numerical results

Figure 1 presents a typical plot of CTOD (Crack Tip Opening Displacement) versus applied load, measured at the first node behind crack tip. Between the minimum load (point A) and point B, the crack is closed. This crack closure phenomenon is produced by the residual plastic wake, formed as the crack propagates, which acts as a plastic wedge forcing the contact of crack flanks. After opening, at point B, the material deforms elastically, up to point C. Then, plastic deformation starts and increases up to point D, corresponding to the maximum load. The plastic CTOD range, δ_p, indicated in Figure 1, is assumed to be the crack driving force for FCG.

Figure 2 shows the effect of the different material constants on FCG rate. Parametric variations of ±25 and ±50% were made in each material parameter, relatively to the reference values presented in Table 2. A linear variation of da/dN with 1/E is evident, which is according with the literature models presented in Table 2. This is a good indication for the robustness of the numerical procedure followed in here. A linear relation can also be accepted for the effect of yield stress, i.e., $da/dN \propto 1/Y_0$. However, for the hardening parameters the influence is non-linear. This makes the development of numerical models more difficult. The effect of C_x and C_y, the saturation rates for kinematic and isotropic hardening, respectively, is less relevant then the effect of X_{Sat} and Y_{Sat}, which are the saturation stresses. In order to have materials with reduced FCG rate, it is important to increase E, Y_0 and all hardening parameters. There is a great influence of material on the trends observed, particularly for the kinematic hardening parameters.

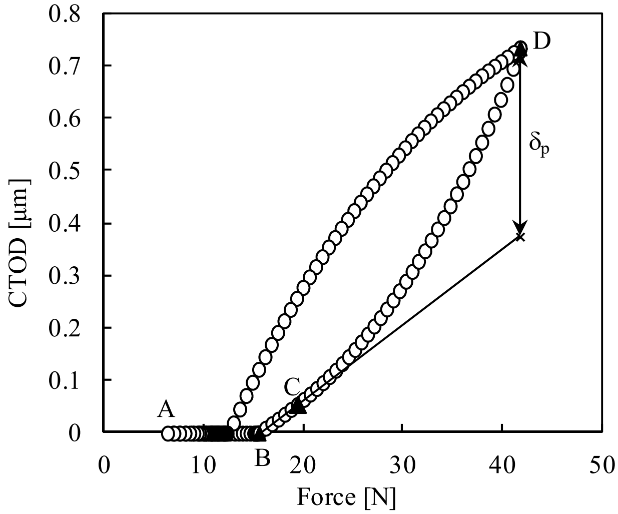

Fig. 1. CTOD versus applied load.

A sensitivity analysis was developed to quantify the relative importance of the different material parameters. The parameters have quite distinct values, therefore a non-dimensional parameter is needed to permit a direct comparison:

$$\nabla f = \frac{\partial \delta_p}{\partial m_p} \cdot \frac{m_p}{\delta_p}, \tag{3}$$

being ∇f the sensitivity coefficient and m_p the material parameter. The elasto-plastic properties studied regarding the variation of plastic CTOD were: Young´s modulus (E), kinematic hardening parameters (C_X and X_{Sat}), and isotropic hardening parameters (Y_0, Y_{Sat} and C_Y). A sensitivity of 0.5 indicates that a variation of 1% in m_p produces a variation of 0.5% in δ_p. Figure 3 shows the non-dimensional sensitivity of δ_p relatively to the different material parameters. There is a great sensitivity of δ_p to material properties, being in general higher than one. The influence of the different parameters is quite variable, ranging from 0,36 for C_Y to 2.6 for Y_0 in Figure 3a. When the contact of crack flanks is removed, the sensitivities vary significantly. The results presented are valid for a single point of the parametric space and the change of point modifies the sensitivities. Finally, the change of material produces a great variation of sensitivity.

5. Discussion

The results in Figures 2 and 3 are illustrative of the complex influence of material parameters on FCG. Linear relations may be proposed for the influence of Young's modulus and yield stress, however non-linear variations are observed for the other material parameters. The relatively importance of material parameters is quite variable and changes with the point of parametric state, crack closure and material. The loading, environment (temperature and atmosphere) and the geometry of the component are additional parameters and so:

$$\frac{da}{dN} = \tilde{f}(\Delta K, K_{max}, E, Y_0, X_{Sat}, C_x, Y_{Sat}, C_y, T, a, t, W) \tag{4}$$

being *a* the crack length, *T* the temperature, *W* the width and *t* the thickness of specimen or component.

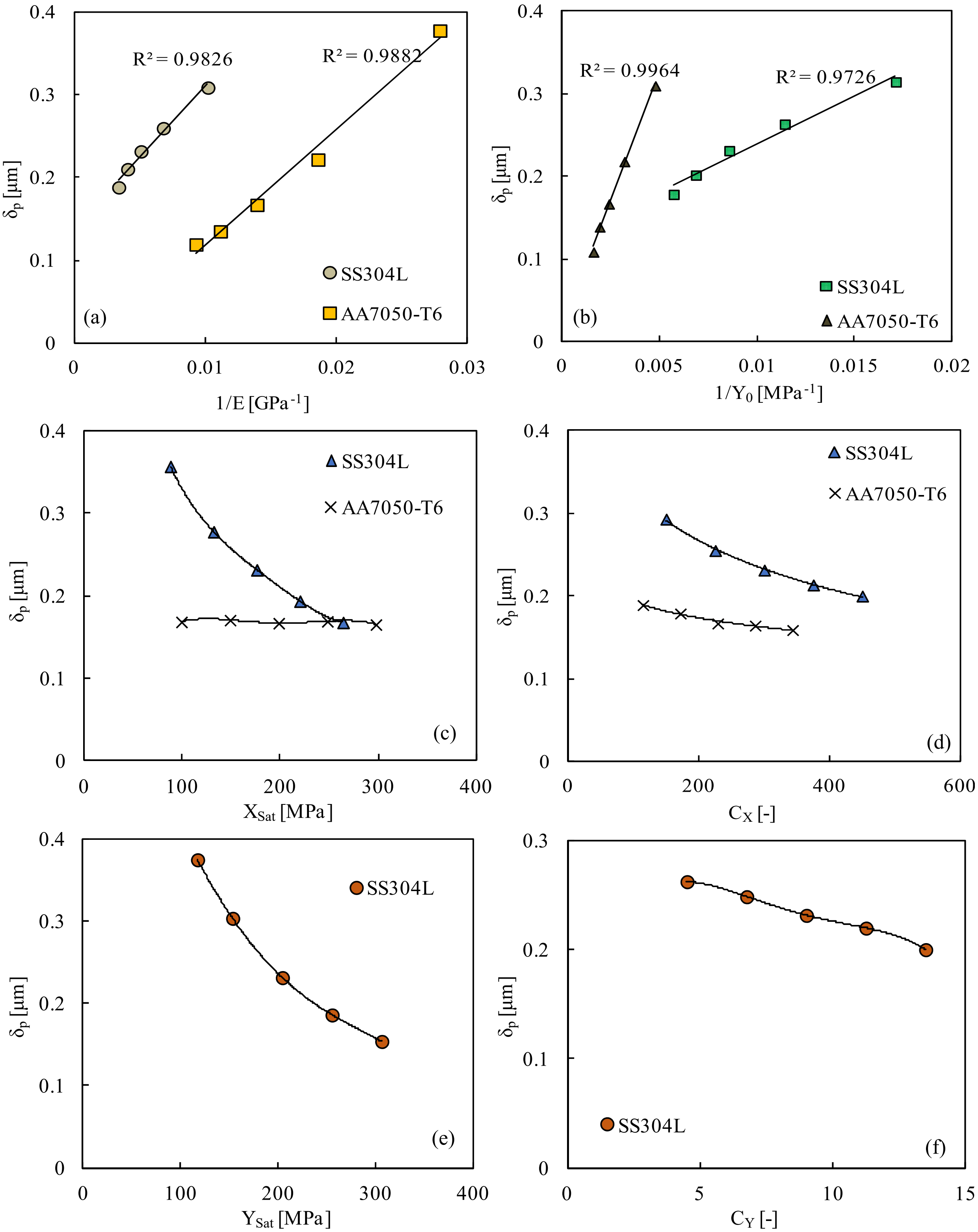

Fig. 2. Effect of material parameters on FCG rate (a) Young's modulus, E; (b) Yield stress, Y_0. (c) Kinematic saturation stress, X_{Sat}. (d) Kinematic saturation rate, C_x. (e) Isotropic saturation stress, Y_{Sat}. (f) Isotropic saturation rate, C_y.

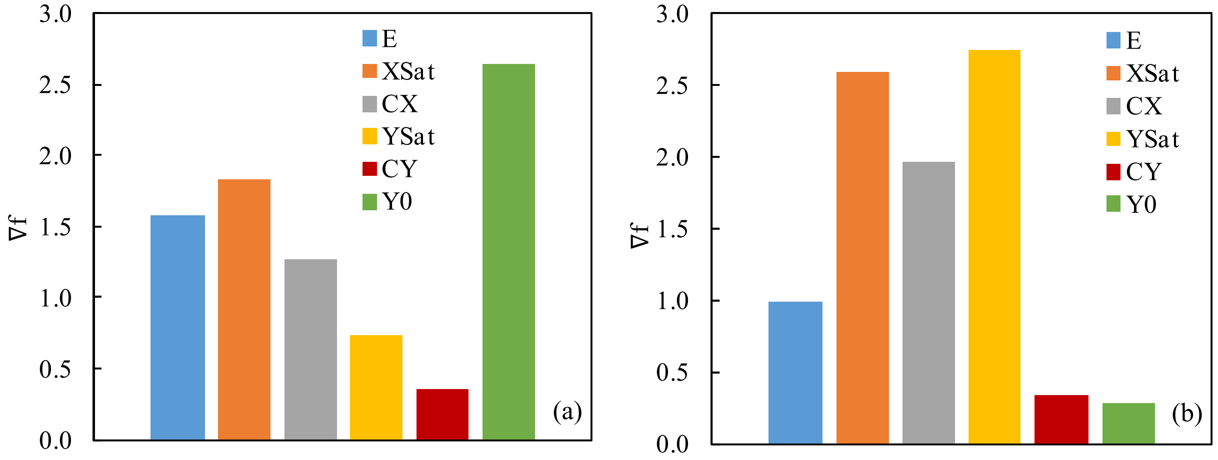

Fig. 3. Non-dimensional sensitivity for the 304L stainless steel. (a) Crack flanks with contact; (b) Crack flanks without contact (a_0=24 mm; 304L stainless steel).

Therefore, it is not easy to develop an analytical model able to accommodate all this complexity. The great number of models proposed in literature, illustrated in Tables 1 and 2, is a consequence of this complexity. In order to reduce the number of parameters, several authors proposed non-linear parameters using dimensional analysis (Carpinteri, 2007):

$$\frac{Y_0^2}{K_{Ic}^2}a;\frac{\Delta K}{K_{Ic}};R;\frac{Y_0^2}{K_{Ic}^2}d \tag{5}$$

being d the grain size and K_{Ic} the fracture toughness. Anyway, this approach does not eliminate the complexity of the problem.

In here, a more fundamental approach is proposed based on the use of CTOD. First, a material law is obtained relating da/dN with plastic CTOD range, δ_p, assuming that this parameter is the crack driving force. Standard MT or CT specimens are used to obtain da/dN and δ_p. Crack length is measured on one side using an optical lent, and the CTOD is measured on the opposite side using Digital Image Correlation. Alternatively, δ_p may be predicted numerically using the finite element method, in simulations which replicate the experimental procedure. Linear relations were obtained using DIC and FEM, therefore the law da/dN-δ_p is dimensionally correct (Antunes, 2017, 2018). The design of a specific component is subsequently made using a numerical analysis. The design of components is nowadays based on CAD tools, therefore these geometrical models may be used as a fast numerical analysis. This analysis includes in a natural way the geometry of component and loading parameters.

6. Conclusions

A short literature review was made about numerical models including load and material parameters on fatigue crack growth. A great number of models have been proposed, for different materials and loading conditions. A numerical analysis was subsequently developed in CT specimens made of 304L stainless steel. The results showed a complex influence of material parameters on FCG. The relatively importance of material parameters is quite variable and changes with the point of parametric state, crack closure and material. The loading, environment (temperature and atmosphere) and the geometry of the component are additional parameters.

Therefore, instead of analytical models, we propose a strategy based on plastic CTOD for the design of components. A material law must be first obtained relating da/dN with plastic CTOD range, δ_p, assuming that this is the crack driving force. δ_p, may be obtained numerically using the finite element method or experimentally using Digital Image

Correlation. This law is specific for each material, therefore includes all material properties. The design of a cracked component is proposed to be made numerically, in order to determine δ_p for different crack lengths. The geometrical and loading parameters are included in a natural way. The fatigue life is obtained integrating the da/dN versus *a* relation.

Acknowledgements

The authors would like to acknowledge the sponsoring under the project no. 028789, financed by the European Regional Development Fund (FEDER), through the Portugal-2020 program (PT2020), under the Regional Operational Program of the Center (CENTRO-01-0145-FEDER-028789) and the Foundation for Science and Technology IP/MCTES through national funds (PIDDAC). The authors also acknowledge the Center of Mechanical Engineering, Material and Processes- CEMMPRE.

References

Antunes, F.V., Branco, R., Prates, P.A., Borrego, L., 2017. Fatigue crack growth modelling based on CTOD for the 7050-T6 alloy. Fatigue Fract Engng Mater Struct 40, 1309-1320.

Antunes, F.V., Díaz, F.A., Vasco-Olmo, J.M., Prates, P., 2018. Numerical determination of plastic CTOD. Fat Fract Engng Mater Struct, 2018; 1–11.

Carpinteri, A., Paggi, M., 2007. Self-similarity and crack growth instability in the correlation between the Paris' constants. Engng Fracture Mechanics 74, 1041–1053.

Chand, S. Garg, S.B.L. 1985. Crack propagation under constant amplitude loading. Engng Fracture Mechanics 21(1) 1-30.

Clavel, M., Pineau, A., 1982. Fatigue behaviour of two Nickel-base alloys I: Experimental results on low cycle fatigue, fatigue crack propagation and substructures. Mater Science and Engng 55, 157-171.

Erdogan, F. and Ratwani, M., 1970. Fatigue and fracture of cylindrical shells containing circumferential crack. Int. J. Fracture Mech. 4, 379–392.

Forman, R. G., Kearney, V. E., Engles, R.M., 1967. Numerical analysis of crack propagation in cyclic loaded structures. Int. J. Fracture Mech. 89, 459–464.

Jablonski, D.A., Carisella, J.V. Pelloux, R.M., 1977. Fatigue crack propagation at elevated temperature in solid solution strengthened superalloys. Mettalurgical Transaction A 8A, 1893-1900.

Kujawski, D., 2001. A fatigue crack driving force parameter with load ratio effects. International Journal of Fatigue 23, S239–S246.

Kwofie S., Rahbar N., 2011. An equivalent driving force model for crack growth prediction under different stress ratios. Int J Fatigue 33, 1199–1204.

NASGRO, 2016, Fracture Mechanics and Fatigue Crack Growth Analysis Software.

Nicholls, D.J., 1994. The relation between crack blunting and fatigue crack growth rates. Fatigue and Fracture of Engng Materials and Struct 17 (4), 459-467.

Pelloux, R.M., 1970. Crack extension by alternating shear. Engng Fracture Mechanics 1, 697-704.

Raju, K. N., 1972. An energy balance criterion for crack growth under fatigue loading from considerations of energy of plastic deformation. Int. J. Fracture Mech. 8, 1–14.

Schwalbe, K.H., 1974. Comparison of several fatigue crack propagation laws with experimental results. Engng Fracture Mechanics 6, 325-341.

Shi, K.K., Cai, L.X., Chen, L., Wu, S.C., Bao, C., 2014. Prediction of fatigue crack growth based on low cycle fatigue properties. International Journal of Fatigue 61, 220–225.

Skelton, R.P., Vilhelmsen, T., Webster, G.A., 1998. Energia Criteria and cumulative damage during fatigue crack growth. Int Journal of Fatigue 20(9), 641-649.

Walker, K., 1970. The effect of stress ratio during crack propagation and fatigue for 2024-T3 and 7075-T6 aluminum. ASTM STP 462, 1–14.